

# **New Empirically-Derived Solar Radiation Pressure Model for GPS Satellites**

Y. Bar-Sever and Da Kuang, Jet propulsion Laboratory, Pasadena, CA 91109

Solar radiation pressure force is the second largest perturbation acting on GPS satellites, after the gravitational attraction from the Earth, Sun, and Moon. It is the largest error source in the modeling of GPS orbital dynamics. Various efforts have been made by different investigators using different approaches to study and develop high precision GPS solar radiation pressure models, essentially for precise orbit determination application [Fliegel et al, 1992, Beutler et al, 1994, Kuang et al, 1996, Fliegel and Gallini, 1997, Bar-sever, 1997, Ziebart, 2002]. Because of the complex GPS satellite surface properties, unobserved satellite attitude variations and weak sensitivity to the satellite perturbation by the tracking data from the Earth, many of the practical solar radiation pressure models for GPS use simplified mathematical functions with coefficients estimated to optimize the tracking data fit. This study is a follow up investigation to the work reported by Bar-Sever [1997], the same approach is used here to derive a solar radiation pressure model from GPS orbit data fit. To refresh our memory, we list the four steps of the approach here:

- 1). Selecting daily "truth" orbit data for consecutive days and form 10-day orbit arcs,
- 2). Fitting each 10-day arc orbit data with a model function and estimating the parameters,
- 3). Combining all satellite arc solutions into one set of model parameters for Block IIA and Block IIR satellites, respectively,
- 4). Evaluating the result model with orbit data fit and prediction tests.

With extended period of orbit data covering from January of 1998 to June of 2002, we derived a new solar radiation pressure force model for Block IIR GPS satellites, and also improved the existing solar radiation pressure force model for Block IIA GPS satellites. These models show improved ability to fit orbit data better over long orbit arc, as well as the ability to predict the orbit with better accuracy. In addition to building the data processing capability for routine model development and updating, we also made considerable effort in analysis aspect, extracting the characteristics from the model parameters and tracking down to possible physical causes. These efforts laid a foundation for future development, possibly of a new generation of physical model.

## **1. Selection of Orbit Data**

The basic idea of building a solar radiation pressure model from orbit data is to fit the truth orbit data dynamically over a long orbit arc, and solve for the dynamic parameters that characterize the solar radiation pressure forces. The "truth" and "long arc" here are relative. Our truth orbit here is the daily orbit solved from global tracking data. Although with imperfect force model, the effect of the dynamic errors on orbit is compensated by daily adjustment of the initial conditions and estimation of stochastic perturbation. When concatenated together, these daily orbits represent a truth orbit over multi-day arc. In integration over a 10-day "long arc" orbit, effect of dynamic errors will accumulate significantly. In order to fit the truth orbit well over a 10-day arc, a good dynamic model has to compensate the dynamic error, so we can develop a good model through the minimization of the long-arc orbit fit.

The GPS orbit derived from the ground tracking data is most accurately presented in the Earth-fixed system, while the Earth Orientation Parameters (EOP) are solved simultaneously. The

dynamic orbit integration is carried out most conveniently in an inertial system. The orbit position presented in J2000 inertial system includes the effect of EOP errors. To minimize this error, we use the best known EOP values, the VLBI-based IERS Bulletin-B values, to transform the truth orbit from the Earth-fixed system into the J2000 inertial system. Table 1 lists the comparison between two sets of orbits in J2000 inertial system, one transformed using Bulletin-B EOP value, the other using the EOP solved from the GPS tracking data. We tested the orbit overlap difference for two weeks, the RMS show consistently that the orbit transformed using Bulletin-B EOP values is more accurate. The RMS values of those orbits transformed to J2000 system using Bulletin-B EOP are essentially the same as the overlap RMS of orbits in the Earth-fixed system.

Table 1. Daily orbit overlap RMS in J2000 inertial system.

Time Span	Bulletin-B EOP derived J2000			GPS-EOP derived J2000		
	H(cm)	C(cm)	L(cm)	H(cm)	C(cm)	L(cm)
98jul01-98jul07	2.7	4.3	6.3	2.7	11.7	12.3
02jul01-02jul07	2.1	2.3	2.8	2.1	11.3	11.5

In order to make a comprehensive orbit data pool for the solar radiation pressure model building, we searched through all daily orbit solutions from January 1, 1998 through July 1, 2002, picking up all the consecutive 10 day arcs that has daily 3D orbit overlap RMS better than 20 cm. We found a total of 2414 arcs, as categorized in Table 2. These orbit data are used in two separate groups, one for Block IIA satellites and the other for Block IIR satellites. Orbit fitting results in each group are combined into a separate set of solar radiation pressure model parameters.

Table 2. Number of 10-day orbit arcs selected for orbit fit.

	Block IIA	Block IIR
Number of Satellites	17	6
Non-eclipsing Arcs	1723	289
Eclipsing Arcs	334	68

## 2. Model Parameterization and Combination of Group Solutions

Our solar radiation pressure force model is a set of mathematical functions. We limit the choice of functions based on reasonable physical assumption. If the GPS satellite solar panel surface always face the Sun perfectly as designed (the nominal yaw and pitch) and the satellite body is a sphere, then the solar radiation pressure force on the satellite would simply be a constant in the Sun-satellite direction. The variation of the force due to the non-spherical satellite body depends only on the relative position among the Earth, satellite and the Sun, namely, the  $\epsilon$  angle as shown in Figure 1.

A frame in which the solar radiation pressure force is most naturally described is the coordinate system tied to the nominal solar panel surface orientation. We refer to this system as UVW system, with U pointing from the satellite to the Sun, V in the solar panel beam direction, and W completing the right hand system. V is in the same direction as the conventional GPS body-fixed Y direction, as shown in Figure 2.

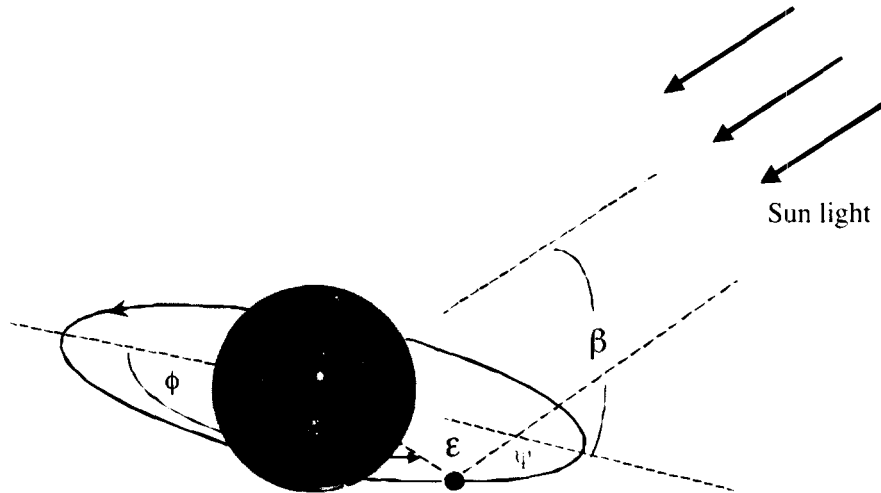


Figure 1. The Earth-Probe-Sun geometry.

Thus we define our model as a function of  $\epsilon$  angle only. We limit our search to low order Fourier expansion of  $\epsilon$  angle. By experimenting with the Fourier expansion terms to minimize the orbit data fit RMS and the correlation between estimated model parameters, we picked this set of functions:

$$F_u = C_U(0) + C_U(1) \cos \epsilon + C_U(2) \cos 2\epsilon \quad (1)$$

$$F_v = C_V(0) + C_V(1) \cos \epsilon + C_V(2) \cos 2\epsilon \quad (2)$$

$$F_w = C_W(1) \cos \epsilon + S_W(1) \sin \epsilon + C_W(2) \cos 2\epsilon \quad (3)$$

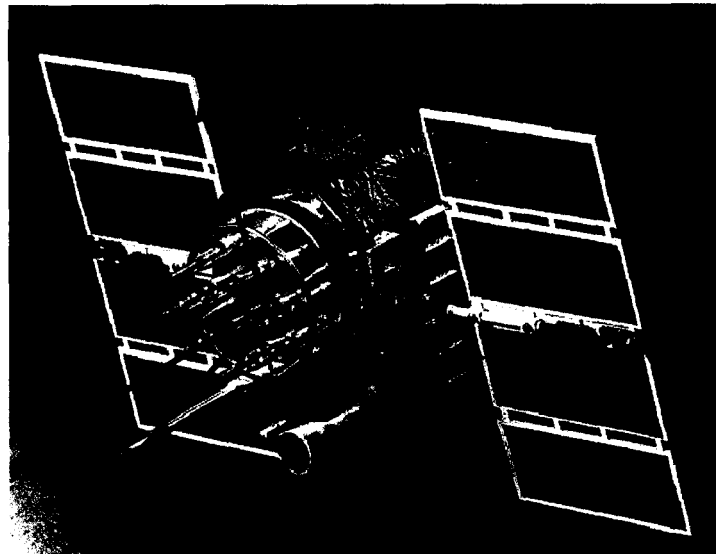


Figure 2. GPS satellite attitude and body-fixed system.

The change of solar flux constant will cause a small variation in the force, change of satellite mass also cause small variation in the perturbing acceleration. These small changes are absorbed into the model parameter estimation in each individual satellite-arc fit. We can think each satellite-arc solution as a slightly scaled sample of the "truth" model. To make a robust estimation of the "truth" model from all the individual samples, we need to combine all the arc solutions with the scale factor accounted for. This is a problem similar to free network estimation problem, without adequate a-priori information there would be no unique solution (see Appendix A). However, from previous description of the solar radiation pressure force model, we know that the  $C_U(0)$  is the main force term, it would be the only term in an ideal situation. And we know that the scale factor, caused by the change of solar flux constant and satellite mass, is in a small neighborhood around 1. Thus it is reasonable to assume that the scale factor is only related with  $C_U(0)$ , and that the expected value of scale factor is 1. With these constrain, we can carry out the combination process in following steps:

- 1). Find the weighted mean of  $C_U(0)$  for all satellite-arc solutions,  $CU_0$ ;
- 2). Scale the parameter vector from each satellite-arc solution to the plane  $C_U(0) = CU_0$ ;
- 3). Find the weighted mean of all the scaled vectors in that plane, the result is the combined parameter vector, as shown in Figure 3.

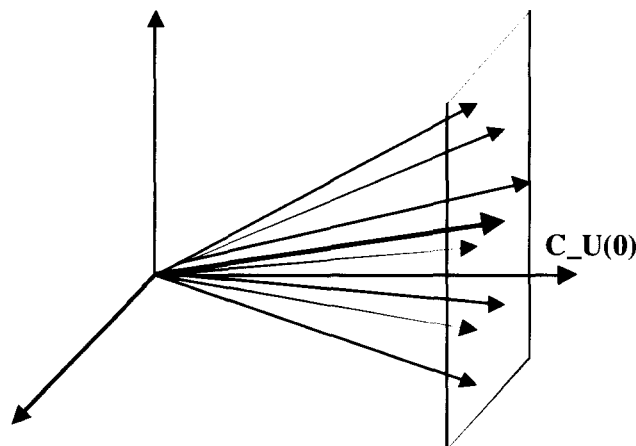


Figure 3. Combination of the model parameter vectors.

When this combined model is applied back to orbit data fit or orbit determination process, a scale factor should be adjusted from the data. Also should be adjusted is the  $C_V(0)$  term, which is same as the conventional Y-bias term.

### 3. Fitting Results and Model Evaluation

The individual satellite-arc solutions are divided into two groups: Block IIA and Block IIR. Combination of each group yields a set of model parameters. Parameter  $C_V(0)$ , the Y-bias, is excluded from the combination process. We also exclude from the combination process the parameter  $C_V(1)$ , which shows significant dependence on  $\beta$  angle. Instead, we fit the  $C_V(1)$  parameter separately with a function of  $\beta$ . Values of combined model parameters are summarized in Table 3.

Table 3. Values of combined Solar Radiation Pressure model parameters.

Parameters	Block IIA	Block IIR
$C_U(0)$	8.881E-5 Newton	11.190E-5 Newton
$C_U(1)$	0.067	0.553
$S_U(2)$	-0.008	-0.243
$C_W(1)$	-0.120	-0.167

S_W(1)	0.011	-0.060
C_W(2)	0.036	0.025
C_V(2)	0.188E-9 m/sec <sup>2</sup>	0.061E-9 m/sec <sup>2</sup>
C_V(1)	0.083+0.556sinβ+0.273/sinβ	-0.008+0.181sinβ+0.097/sinβ

To test this newly derived model, we apply the combined model back in the orbit data fit by fixing the above parameter values and estimating a solar radiation scale factor and Y-bias values for each solution. Figure 4 and Figure 5 show the improvement of the average data fit RMS by the new model over the existing model. For Block IIA satellites, the old model is also an orbit data derived model, but from smaller database. The data fit RMS improvement is about 5 cm. For Block IIR satellites, the improvement is much more significant, because the old model is the ROCK4 type model derived from ground test data. The new model is the first flight data derived model for Block IIR satellites.

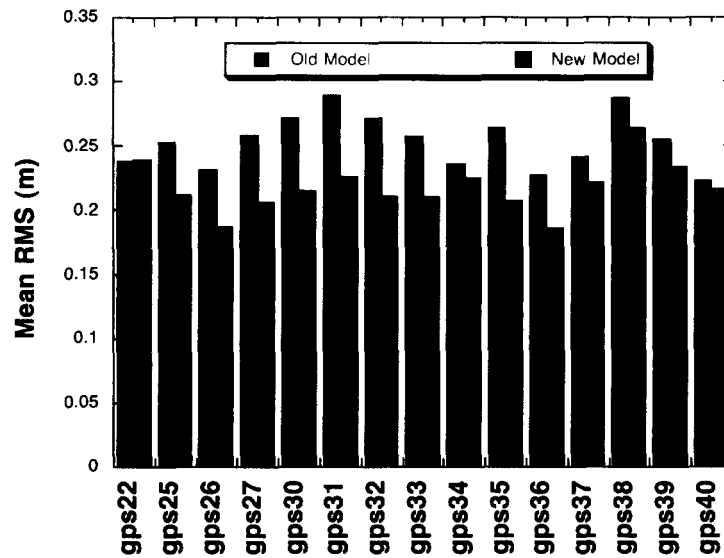


Figure 4. Average 10-day arc orbit data fit RMS for Block IIA satellites.

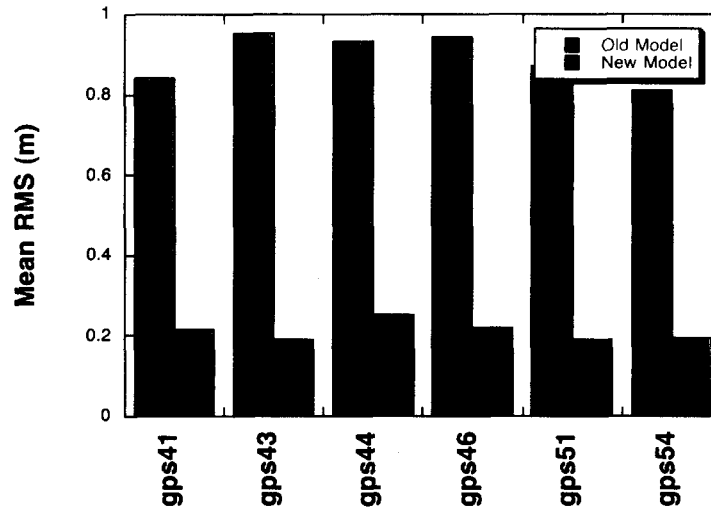


Figure 5. Average 10-day arc orbit data fit RMS for Block IIR satellites.

The new model is also test for its prediction power. In the prediction test, we fit 4-day arc of orbit data, then integrate forward another 4 days using the initial status and force parameters (solar radiation scale factor and Y-bias) estimated from the data fit. The RMS of the difference between the predicted orbit and the truth orbit on the end day is computed as the prediction error. The average prediction RMS improvement is summarized in Figure 6 and Figure 7. Again, the improvement for Block IIR satellites is more significant, and with the new model, the average prediction error for both Block IIA and Block IIR satellites are on the same level.

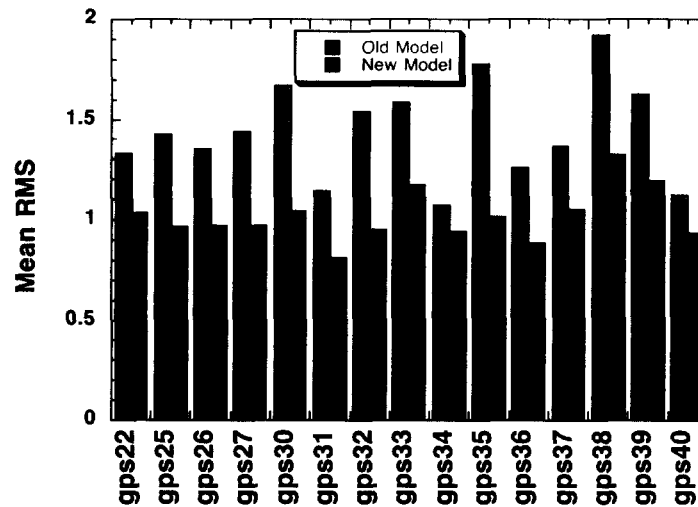


Figure 6. Average 4-day prediction RMS for Block IIA satellites.

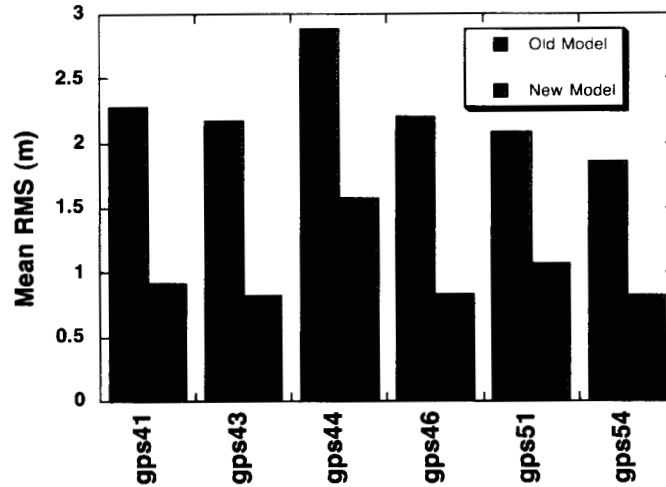


Figure 7. Average 4-day prediction RMS for Block IIR satellites.

#### 4. Characteristics of the Model Parameters

As mentioned in previous sections, when chose the solar radiation pressure force function, we expected the forces are functions of  $\epsilon$  angle only. Plotting the estimated force parameters of all 10-day arc solutions, we can see that there is linear trend and annual variation. This is not surprising, because the satellite mass decreases constantly and the solar flux constant changes annually. These effects are accounted for by the scale factor in the combination process. However, the estimated parameters also show certain type of trend when plotted against  $\beta$  angle (Figure 8 through Figure 11). These model parameters as functions of  $\beta$  angle demonstrate at least two characteristics. First, most parameters show big formal sigma and wilder deviation values at high  $\beta$  angle region. Secondly, some model parameters show significant  $\beta$  angle dependence. These characteristics need some investigation, because they indicate that there are other factors than the pure Earth-Probe-Sun geometry contributing to the perturbation and these factors were missing from our original consideration when we designed this solar radiation model.

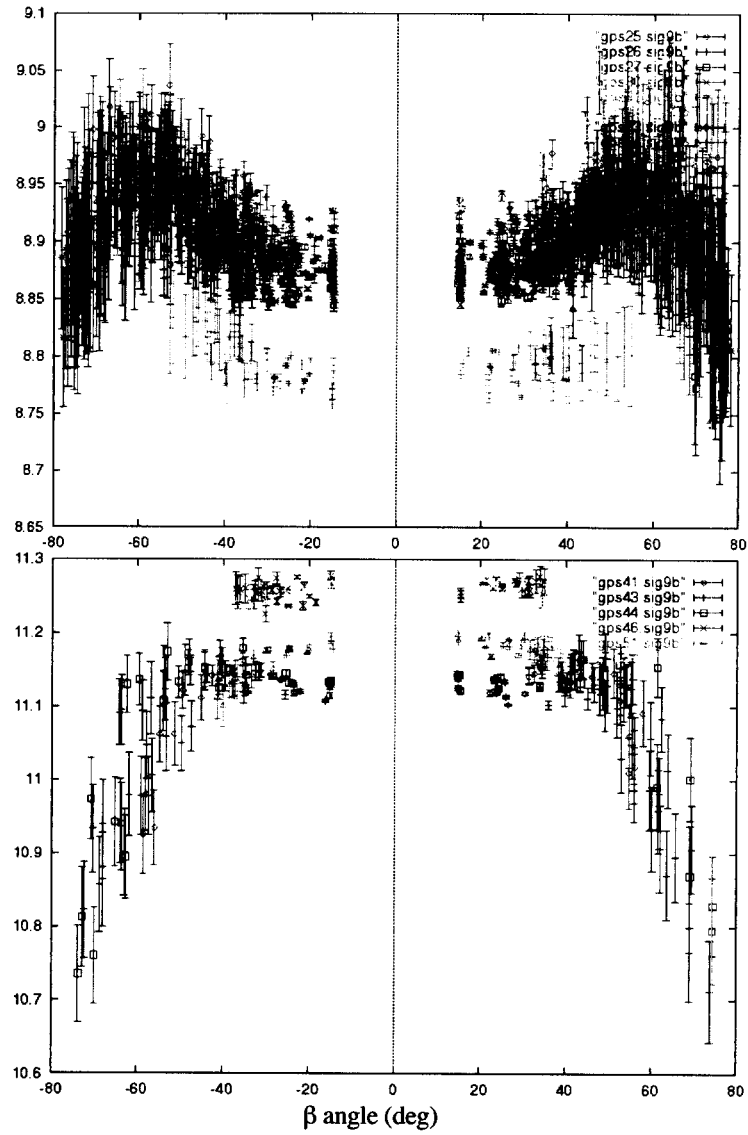


Figure 8. Plot of  $C_U(0)$  as function of  $\beta$ , unit is  $10E-5$  Newton. Upper one is for Block IIA satellite, lower one is for Block IIR satellites.

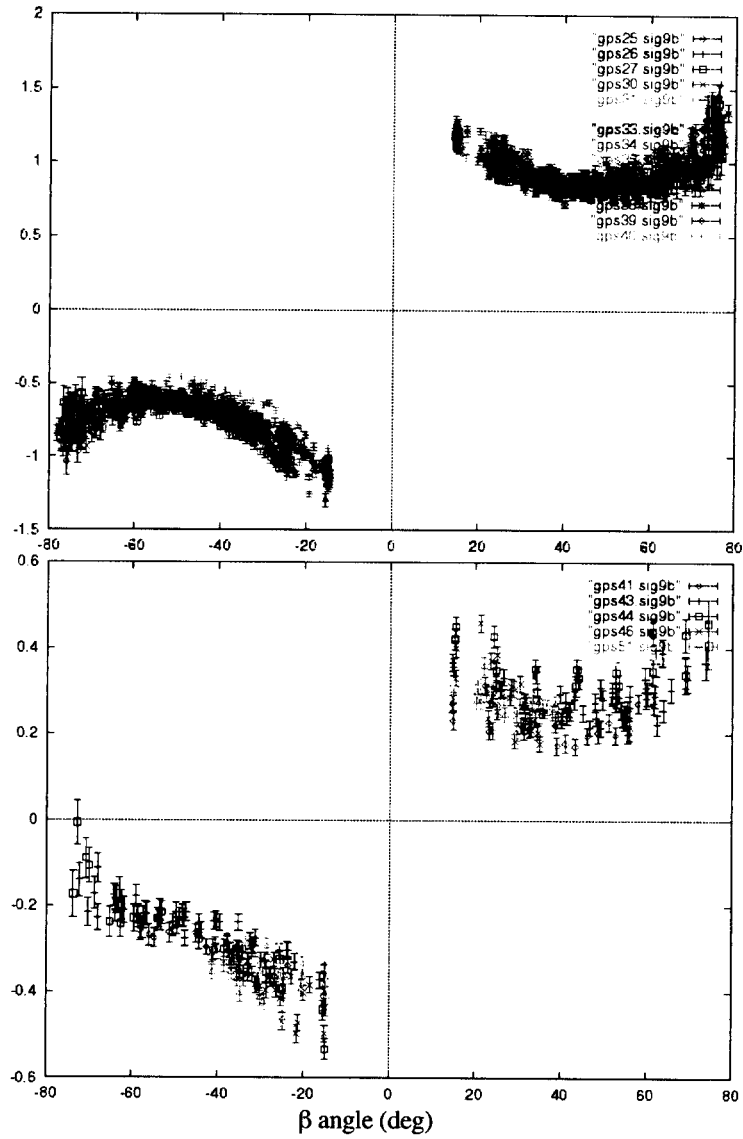


Figure 9. Plot of  $C_V(1)$  as function of  $\beta$ , unit is  $10E-9 \text{ m/sec}^2$ . Upper one is for Block II A satellite, lower one is for Block IIR satellites.

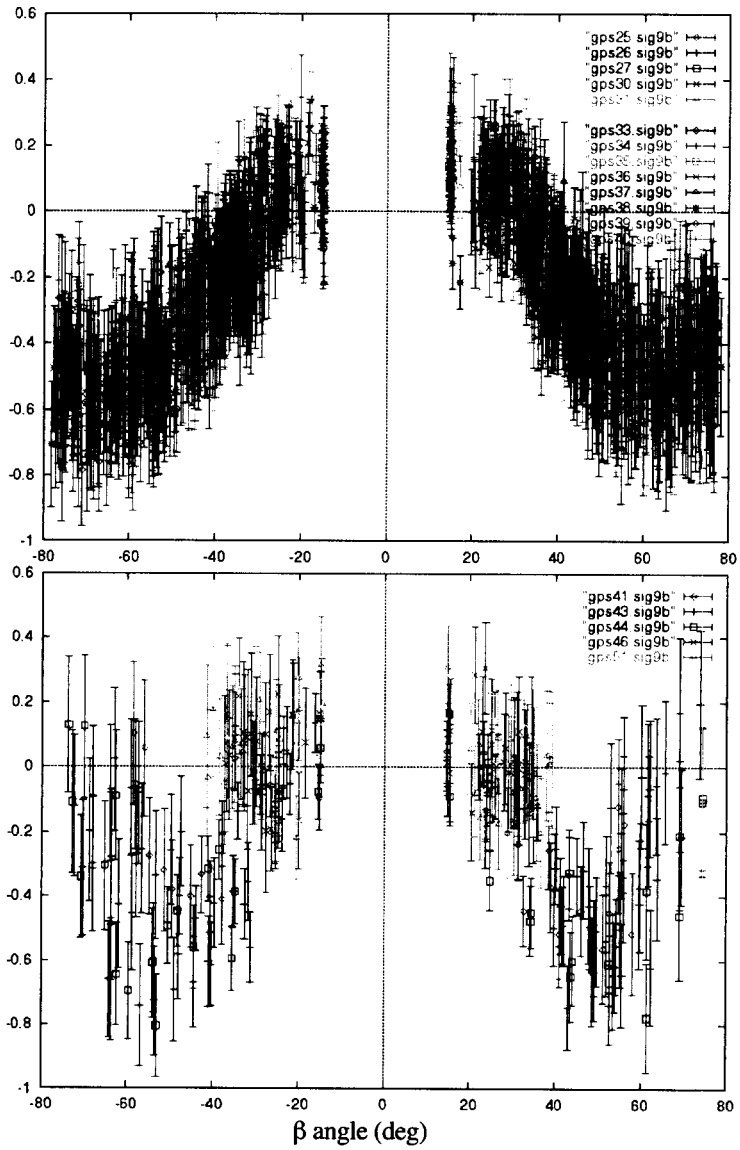


Figure 10. Plot of  $C_W(1)$  as function of  $\beta$ , unit is  $10E-5$  Newton. Upper one is for Block IIA satellite, lower one is for Block IIR satellites.

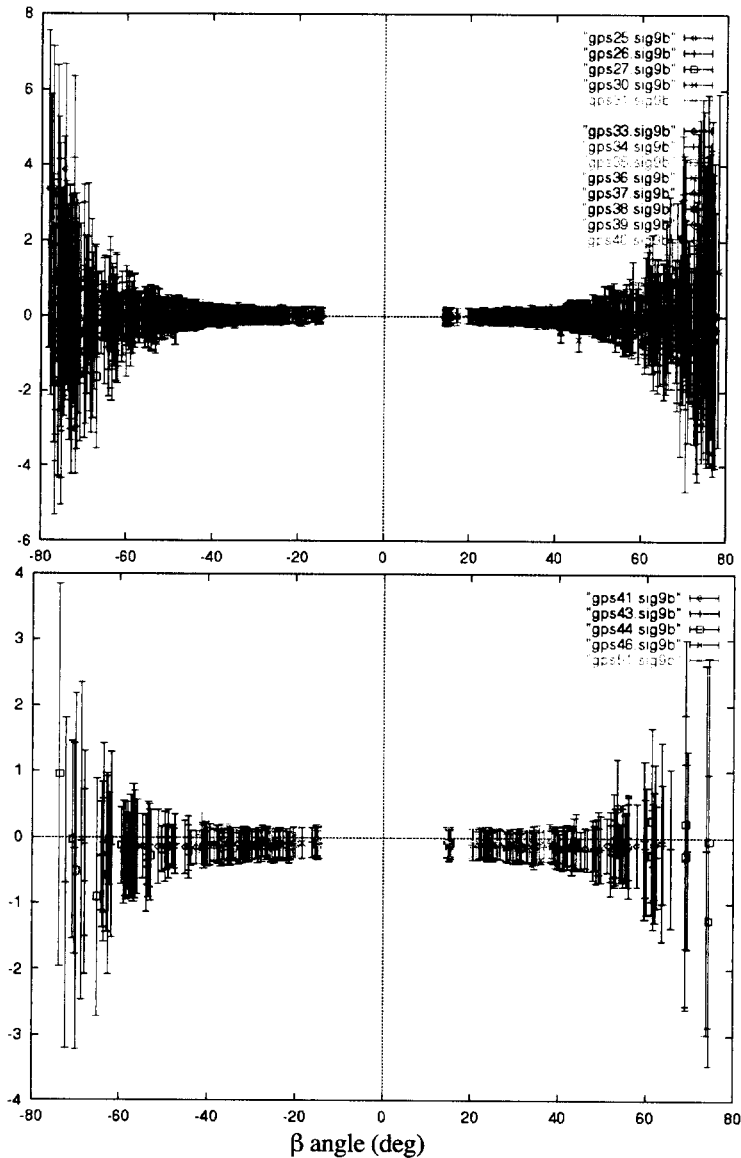


Figure 11. Plot of  $S\_W(1)$  as function of  $\beta$ , unit is  $10E-5$  Newton. Upper one is for Block IIA satellite, lower one is for Block IIR satellites.

There are two possible reasons for the  $\beta$  angle dependency: the sampling effect of the orbital arc and the attitude mismodeling.

### 1) The sampling effect

The  $\epsilon$  angle varies between 0 and 180 degree. However, for each orbital arc, the satellites experience only a subset of the  $\epsilon$  angle. At high  $\beta$  angle region, the  $\epsilon$  angle varies a small amount around 90 degree. On the contrary, at low  $\beta$  angle region, the satellite experience much broader range of  $\epsilon$  angle. The small variation of  $\epsilon$  angle at high  $\beta$  angle region causes poor observability of the function of  $\epsilon$  there. As a result, the solar radiation pressure model parameters that are estimated from high  $\beta$  angle orbit data has larger forma sigma values. In addition, different e variation range gives different mean value of the varying satellite body profile, thus the constant terms and periodic

terms in the Fourier expansion model get different shares of the satellite body profile at different  $\beta$  region. Figure 12 shows the average cross section area of the satellite bodies as a function of  $\beta$  angle, viewed from the Sun's direction. The shape of the function for Block IIR satellite seems a good candidate to explain the  $\beta$  dependency of parameter  $C_U(0)$ .

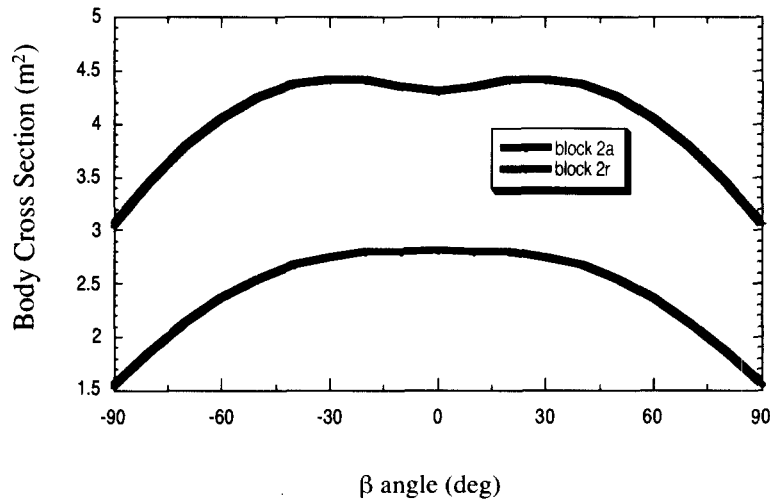


Figure 12. Average body cross section area viewed from Sun direction.

## 2) The effect of attitude mismodeling

Although the Earth-Probe-Sun geometry is only a function of  $\epsilon$  angle, the GPS attitude, namely, the yaw and pitch angles, do depend on  $\beta$  angle. If the satellite attitude is deviated from the ideal situation (the nominal attitude), some perturbation force term would show up, and they may depend on  $\beta$  angle.

Among all the model parameters, the  $C_V(1)$  is the most eye-catching term. It is not only the most significant periodic term in improving the data fit RMS, but also the most odd shaped one that shows discontinuity at  $\beta = 0$  (Figure 9). This perturbation term is consistent with other observations. Kuang et al [1996] noticed that the periodic perturbation forces on GPS satellites recovered from orbit data could be explained by a wobbling of the solar panel around its nominal pointing direction. When the satellite exited an eclipsing season, the wobbling reversed its direction. The change of phase angle in the once per revolution perturbing force has been observed in other studies as well. Figure 13 shows the phase angle of the estimated once per revolution force in cross-track direction during a six weeks period covering April 27-June 7 of 1997. The four satellites are in the same orbit plane, when the  $\beta$  angles change sign, all these satellites show a 180 degree change in the phase angle of the periodical force in cross-track direction. Since for small  $\beta$  angle the Cross-track direction is close to the Y-direction except the sign, what Figure 13 shows is that the once per revolution perturbing force in the solar panel beam direction changes sign when  $\beta$  angle changes sign.

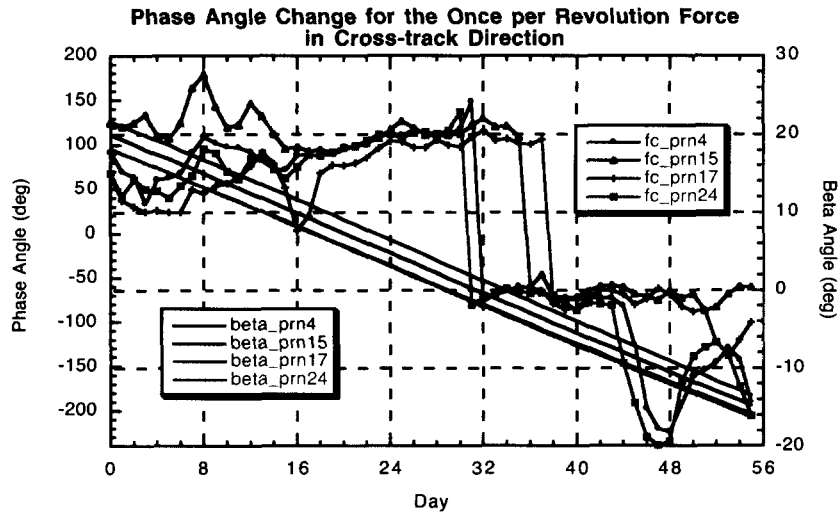


Figure 13. Change of phase angle for once per revolution force in cross-track direction.

It has been shown by Kuang et al [1996] (and reorganized in Appendix B) that a small pointing error of the solar panel in V (or W) direction will produce a small perturbing force in that direction proportional to the pointing error. Thus any perturbation in V or W direction can be interpreted as a solar panel pointing error. Modeling the perturbing force in V or W direction is equivalent to modeling the corresponding pointing error. The question now is what mechanism would produce the pointing error time series as implied by the parameters recovered from the orbit data fitting.

## 5. Possible Yaw Attitude Error

Let's define:

- Orbit angle  $\varphi$  -- angle in orbit plane measured from the midnight point to the satellite;
- Sun angle  $\beta$  -- angle between the Sun direction and the orbit plane;
- Sun-Satellite-Earth angle  $\varepsilon$  -- angle between the Sun and Earth as viewed at the satellite,  
 $|\varepsilon| < 180$  degree;
- yaw angle  $\psi$  -- angle from the orbit plane to the Sun-satellite-Earth plane;
- pitch angle  $\theta$  -- angle in the Sun-satellite-Earth plane, from local horizon to the Sun,  
with same sign as  $\beta$  angle;

With  $\beta$  and  $\varphi$  as the independent variables, these angles can be expressed as:

$$\cos \varepsilon = \cos \beta \cos \varphi \quad (4)$$

$$\sin \psi = \frac{\sin \beta}{\sin \varepsilon} \quad (5)$$

$$\cos \psi = - \frac{\cos \beta \sin \varphi}{\sin \varepsilon} \quad (6)$$

$$\theta = \frac{\pi}{2} - \varepsilon \quad (7)$$

Although the  $\varepsilon$  angle uniquely defines the Sun-Satellite-Earth geometry and pitch attitude, it does not uniquely define the yaw attitude.

By ignoring the change rate of  $\beta$ , the rate of  $\varepsilon$ ,  $\psi$  and  $\theta$  can be calculated as:

$$\begin{aligned} \dot{\varepsilon} &= \frac{\cos \beta \sin \varphi}{\sin \varepsilon} \dot{\varphi} + \frac{\sin \beta \cos \varphi}{\sin \varepsilon} \dot{\beta} \\ &\approx \frac{\cos \beta \sin \varphi}{\sin \varepsilon} \dot{\varphi} = - \cos \psi \dot{\varphi} \end{aligned} \quad (8)$$

$$\begin{aligned} \dot{\psi} &= \frac{\sin \varepsilon \cos \beta \dot{\beta} - \sin \beta \cos \varepsilon \dot{\varepsilon}}{\sin^2 \varepsilon \cos \psi} \\ &\approx \frac{\sin \beta \cos \varepsilon}{\sin^2 \varepsilon} \dot{\varphi} \end{aligned} \quad (9)$$

$$\begin{aligned} \dot{\theta} &= -\dot{\varepsilon} \approx \cos \psi \dot{\varphi} \\ &= - \frac{\cos \beta \sin \varphi}{\sin \varepsilon} \dot{\varphi} \end{aligned} \quad (10)$$

where  $\dot{\varphi}$  is approximately the mean motion of the satellite. If there is a lag in the pitch attitude, by some reason, proportional to the pitch rate, then it will produce a periodical pointing error of the solar panel in the W direction. Similarly, a lag in the yaw attitude proportional to the yaw rate will produce a periodical yaw angle error, and corresponding pointing error in Y direction is the projection of the yaw error to the Y (the solar panel beam) direction:

$$\begin{aligned} \dot{\psi} \cos \theta &= \dot{\psi} \sin \varepsilon \\ &\approx \frac{\sin \beta \cos \varepsilon}{\sin \varepsilon} \dot{\varphi} \end{aligned} \quad (11)$$

Figure 13 shows the cosine of  $\varepsilon$  angle, which is the base of  $C_V(1)$  force, as function of orbit angle  $\varphi$  and  $\beta$  angle. Figure 14 shows the yaw rate projection in Y direction, which is the base of pointing error in V, as function of orbit angle  $\varphi$  and  $\beta$  angle. Figure 15 shows the pitch rate, which is the base of pointing error in W direction.

It is clear that the  $C_V(1)$  base function agrees with the yaw rate quite well in the high  $\beta$  angle region. In lower  $\beta$  angle region the two functions differ, however, this does not make a crucial difference in orbit because the Y direction turns into a dynamically insignificant direction (Cross-track direction) in the lower  $\beta$  angle region. The pitch rate function, on the other hand, does not resemble any of the base functions in the Fourier expansion.

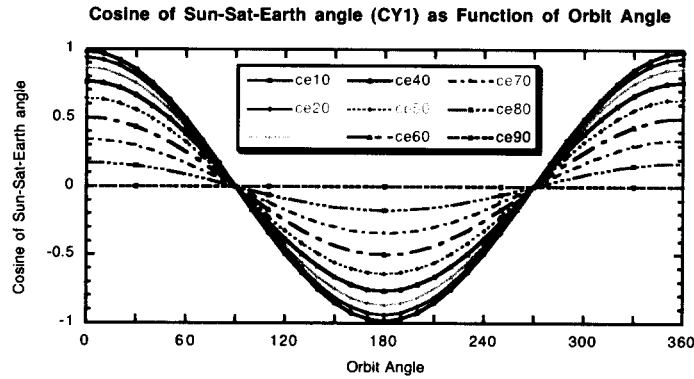


Figure 14. The  $C_V(1)$  base as function of orbit angle and  $\beta$  angle, the 9 curves corresponds to  $\beta = 10, 20 \dots 90$  degree, respectively.

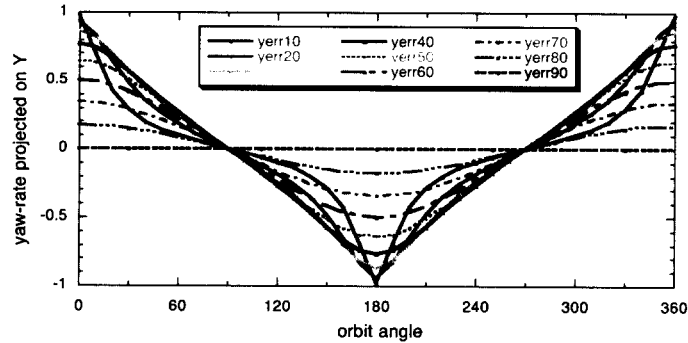


Figure 15. The yaw rate projection in Y direction as function of orbit angle and  $\beta$  angle.

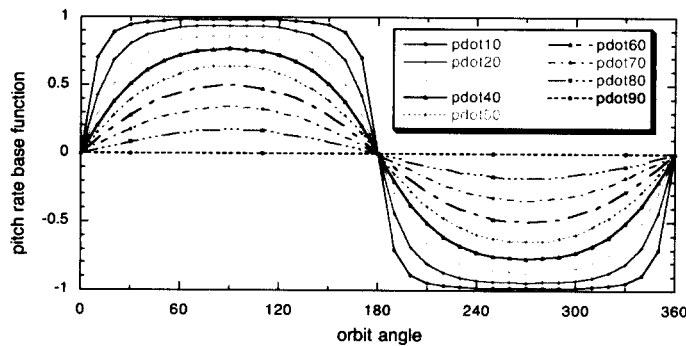


Figure 16. The pitch rate as function of orbit angle and  $\beta$  angle.

To test the hypothesis, we replaced the  $C_V(1)$  term in the model with an acceleration of

$$F_v = f_v \dot{\psi} \sin \varepsilon = f_v \frac{\sin \beta \cos \varepsilon}{\sin \varepsilon} \dot{\varphi} \quad (12)$$

The data fit RMS for the 10-day orbit fit remained almost the same. Figure 17 shows the parameter  $f_v$  estimated from the orbit fit for GPS25.

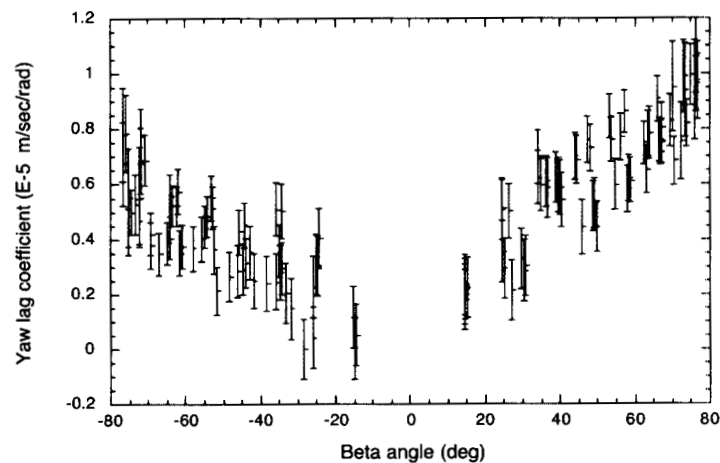


Figure 17. Estimated yaw lag coefficient parameter for GPS25.

Using the value of satellite property parameters for Block IIA satellites given by Fliegel et al., [1992], the average of the above estimated coefficient converts to an attitude lag of 3 minutes. During this lag time, the nominal GPS satellite yaw attitude changes about 0.5 degree at  $\beta$  angle of 40 degree.

## 6. Future Work in Modeling the Solar Radiation Pressure

The approach of developing solar radiation pressure model from the orbit data fit is a flexible and accurate way of model development. As new orbit data becoming available, we can always reprocess the data and derive improved model parameters. The feature of actual in-orbit behavior of satellites can be revealed from the real orbit data fit, and it helps to deepen our understanding of the actual perturbing force and keep improving the model. As we have seen, the Fourier expansion parameters estimated from the orbit data fitting show beta angle dependence, implicating possible attitude model error. The large formal error for parameters in high  $\beta$  angle region reveals the weakness of the Fourier expansion model in that region. Figure 19 and Figure 20 show the base functions  $\cos\epsilon$ ,  $\sin 2\epsilon$ ,  $\cos 2\epsilon$  and  $\sin\epsilon$  over all positive  $\beta$  angle region. The terms  $\cos\epsilon$  and  $\sin 2\epsilon$ ,  $\sin\epsilon$  and  $\cos 2\epsilon$  are highly correlated at high  $\beta$  region. For the future work, we need to find better model parameterization to improve in these areas:

- 1). to remove the discontinuity of parameters at  $\beta = 0$ , and reduce the  $\beta$  angle dependency, so that the model can be easily extended into eclipsing season;
- 2). to reduce the correlation between parameters in the high  $\beta$  value region, so that model parameters can be estimated and combined more robustly.

The success of these tasks relies on understanding the physical reason behind the perturbations. Our analysis in this work has made a good start.

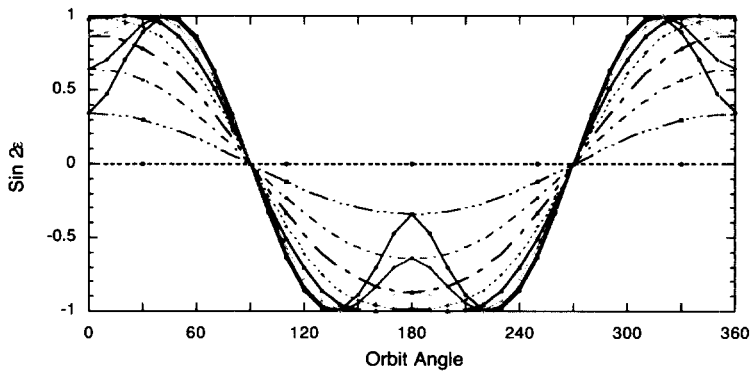
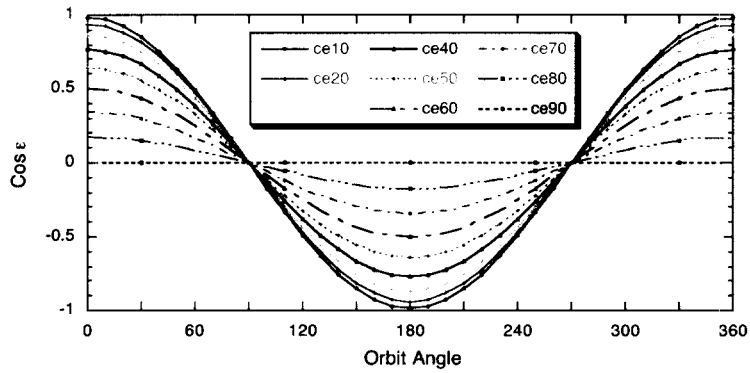
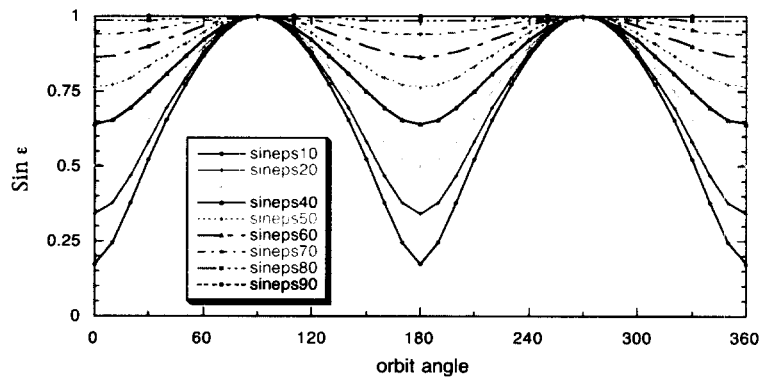


Figure 18.  $\text{Cos } \epsilon$  and  $\text{sin } 2\epsilon$  as function of orbit angle and  $\beta$  angle.



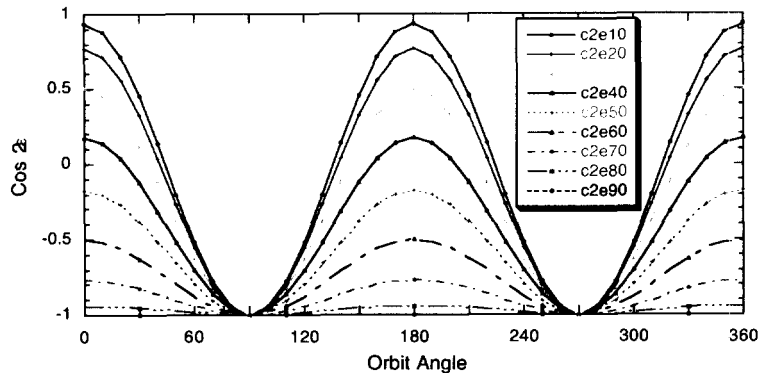


Figure 19.  $\text{Sin}\epsilon$  and  $\text{cos}2\epsilon$  as function of orbit angle and  $\beta$  angle.

## 7. Acknowledgment

The research described in this paper was carried out at the Jet Propulsion Laboratory, California Institute of Technology, under a contract with the National Aeronautics and Space Administration.

## 8. References

Bar-Sever, Y.E., New and Improved Solar Radiation Pressure Models for GPS Satellites Based on Flight Data, JPL Report, 1997.

Beutler, G., E. Brockman, W. Gurtner, U. Hugentobler, L. Mervart, M. Rothacher, and A. Verdun, Extended orbit modeling techniques at the CODE processing center of the International GPS Service for Geodynamics (IGS): theory and initial results, *Manuscripta Geodaetica*, 19, 367-386, 1994.

Fliegel, H.F., T.E. Gallini, and E.R. Swift, Global Positioning System radiation force model for geodetic applications, *J. Geophys. Res.*, 97, 559-568, 1992.

Fliegel, H.F. and T.E. Gallini, Solar force modeling of Block IIR Global Positioning System satellites, *J. Spacecraft and Rockets*, Vol. 33, No. 6, 863-866, 1996.

Kuang, D., H.J. Rim, B.E. Schutz and P.A.M. Abusali, Modeling GPS satellite attitude variation for precise orbit determination, *J. of Geodesy*, 70, 572-580, 1996.

Ziebart, M., P. Cross, and S. Adhya, Modeling photon pressure, the key to high-precision GPS satellite orbits, *GPS World*, Vol. 13, No. 1, 43-50, 2002.